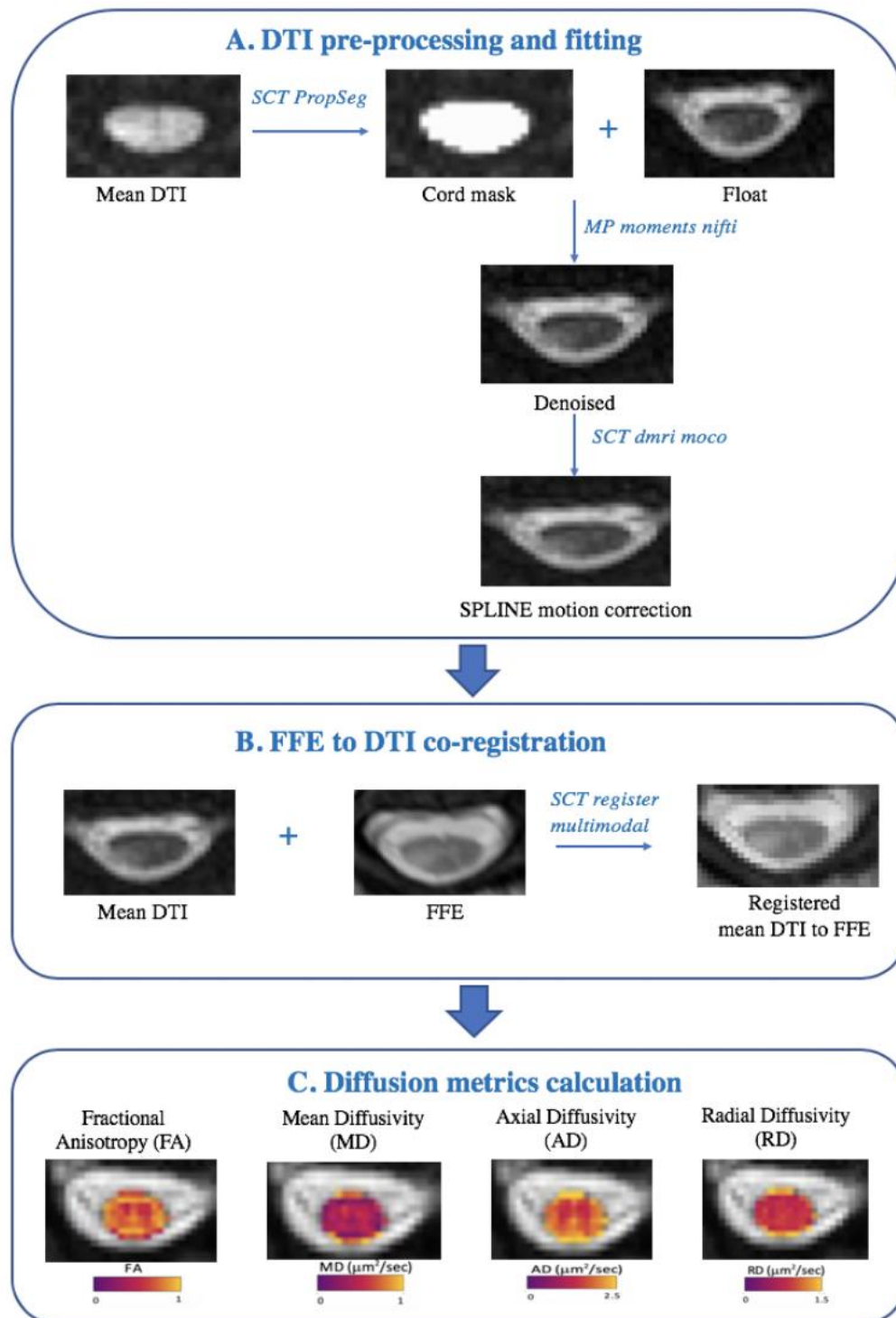


Supplementary Materials:

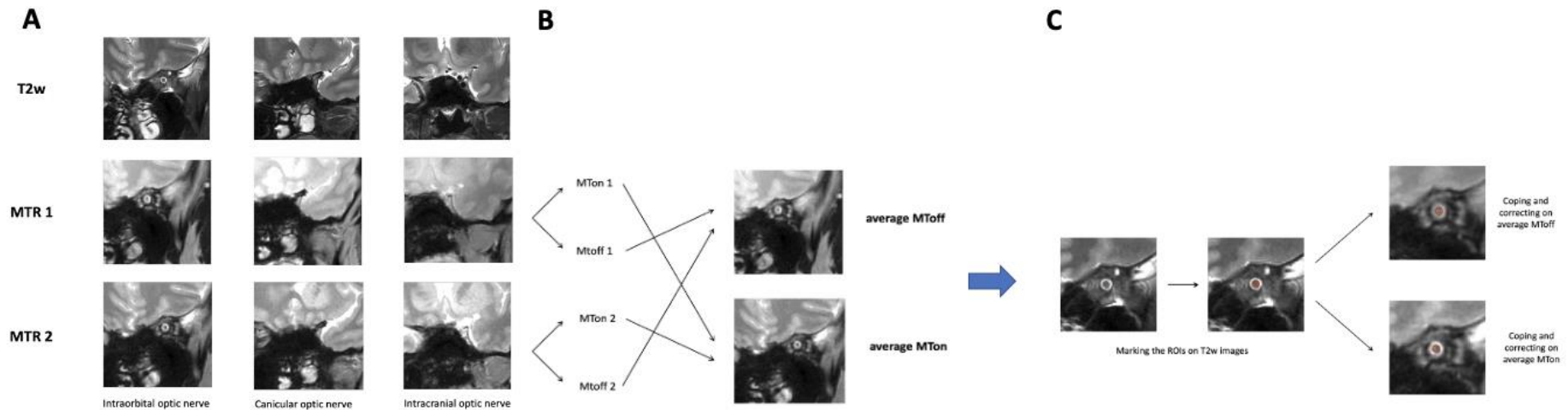
eFigure 1: Diffusion imaging processing pathway



The Figure illustrates the processing pipeline for the diffusion data⁴⁶. (A) Spinal cord was segmented on the mean diffusion-weighted image. The entire diffusion data set was denoised within the spinal cord slice-by-slice with Marchenko-Pastur principal component analysis (MP-PCA) denoising, using an in-house adaptation of freely available Matlab code (https://github.com/NYU-DiffusionMRI/mppca_denoise/blob/master/MP.m). After MP-

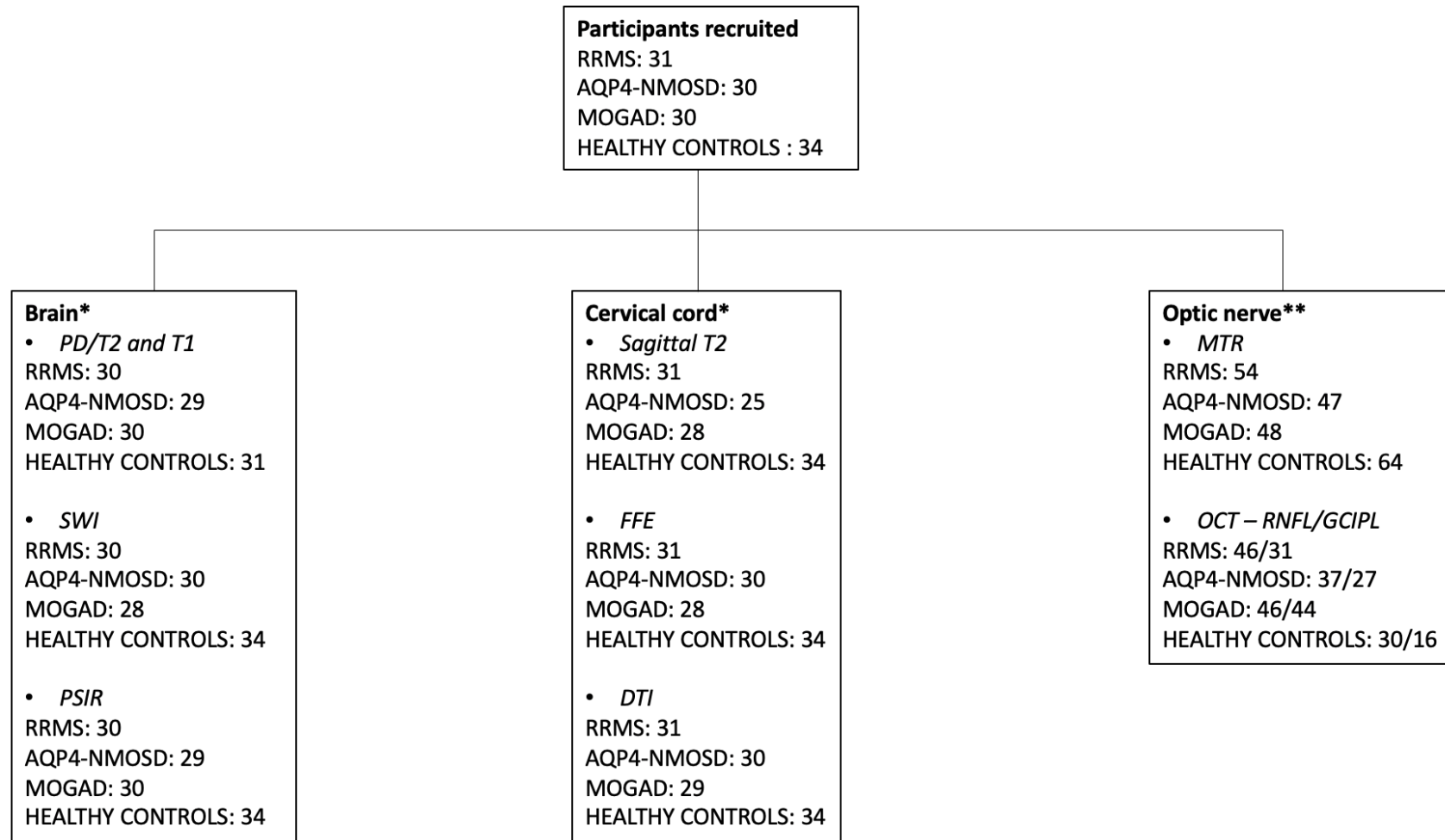
PCA denoising, the noise floor was mitigated using a custom implementation of the method of moments and data corrected for motion. (B) Afterwards, the diffusion tensor model was fit to the motion-corrected data using the DTIFIT function in order to characterise multi directional diffusion of each voxel. The mean diffusion-weighted image, post motion correction, and the FFE image were segmented in order to create cervical cord masks. We used the SCT function, sct_register_multimodal, to calculate the registration transformation and carry out the registration. The deformation is non-rigid and is in the Z direction (axial plane) as the destination orientation of the FFE image was axial. The diffusion weighted images were registered to the anatomical FFE images, as it is favourable to register to the image of best resolution, based on an inversion method (Inverse contrast Normalisation for Very Simple registration). (C) The whole cord mask was used. All masks and DTI metrics were checked and manually corrected using FSL eyes (version 6). The mean values of each diffusion metric (fractional anisotropy [FA], axial diffusivity [AD], mean diffusivity [MD] and radial diffusivity [RD]) within each cord ROI were calculated.

eFigure 2: Optic nerve analysis magnetization transfer ratio (MTR) pipeline



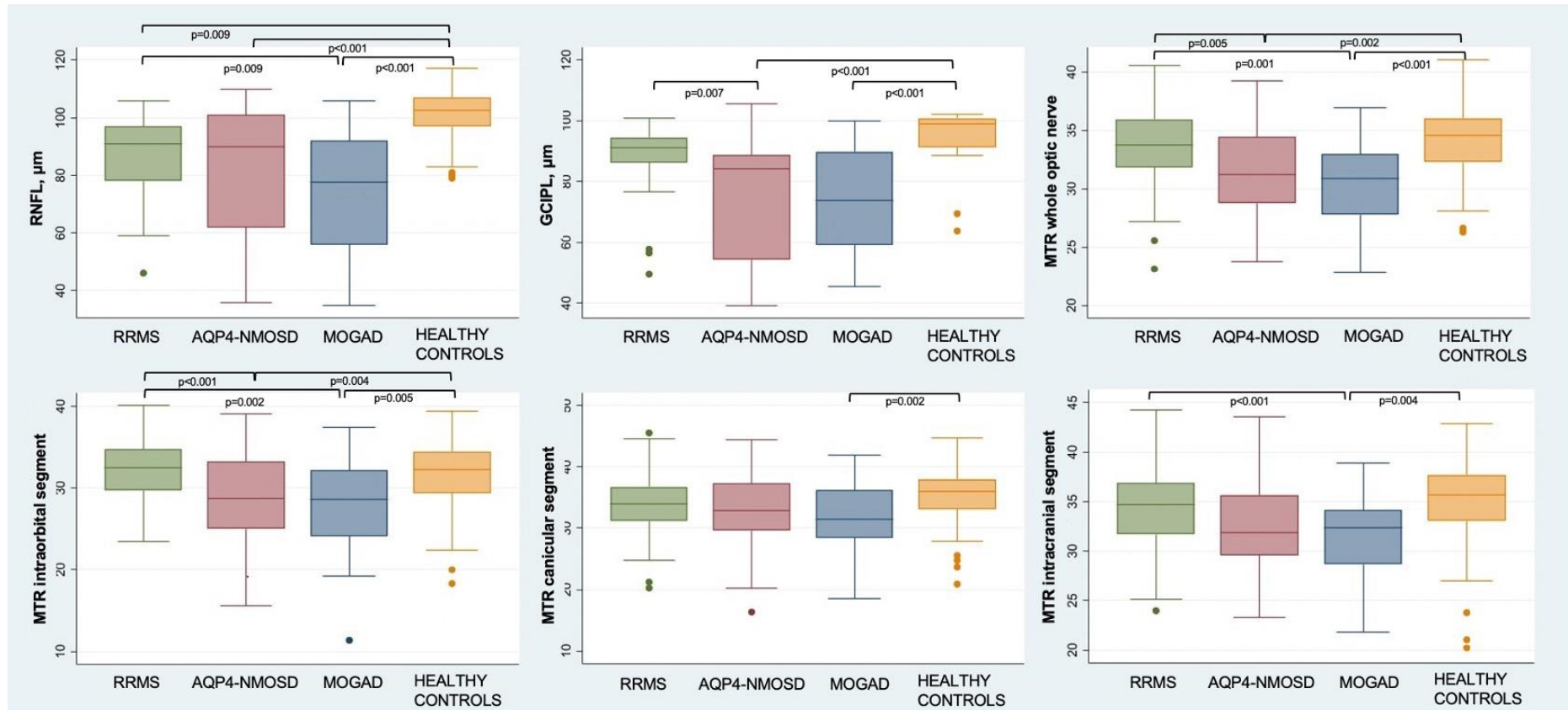
The Figure illustrates the processing pipeline for the MTR optic nerve analysis. (A) Two MT acquisitions (2 echo-times) were obtained for each eye and they were pre-processed to generate two MTON and two MTOFF images. (B) From these two different echo time MT images, average MTOFF and average MTON images were created, which were subsequently pre-registered to the native T2w image. (C) Two raters (R.C. and A.B.) manually delineated slice-by-slice ROIs around the coronal sections of the optic nerves independently on each T2w acquisition (left and right) from anterior orbit to the intracranial part of the nerve inclusive and excluding the CSF surrounding the nerve using JIM 6.0 (Xinapse systems, <http://www.xinapse.com>). Afterwards, these ROIs were transposed onto the pre-registered MTON and MTOFF average images and manually adapted to delineate the same area on the pre-registered MTON and MTOFF average. Subsequently, to correct for small nerve motion, the three ROIs' center-of-mass slice-wise were aligned to a common space (T2 and registered average MTON and MTOFF). This procedure reduced the potential bias introduced by eye motion between scans. Each slice was manually assigned to a specific region of the optic nerve: (0) globe, (1) intra-orbital optic nerve, (2) intra-canicular optic nerve and (3) intra-cranial optic nerve. The average MTR value of each region was calculated considering all the ROIs included in that region.

eFigure 3: Flow chart describing the final number of participants remaining in each group after the quality check of the images



*Refers to patients **refers to eyes.

eFigure 4: Differences in optic nerve measures between RRMS, AQP4-NMOSD, MOGAD and healthy controls.



The boxplots show reduced GC IPL thickness, average MTR of the whole optic nerve and intraorbital segment in AQP4-NMOSD than RRMS patients and reduced RNFL thickness, average MTR of the whole optic nerve, intraorbital and intracranial segments in MOGAD than RRMS patients.

eTable 1: MRI sequences parameters

Sequences*		Repetition time (ms)	Echo time (ms)	Field of view (mm ²)	Voxel size (mm ³)	No. of excitations	No. of slices	Scan time (min)
<i>Brain</i>	Axial PD/T2 - weighted turbo spin-echo (TSE)	3500	15/85	240 x 180	1 x 1 x 3	1	50	4:01
	Sagittal 3D T1 magnetization-prepared gradient-echo sequence	6.9	3.1	256 x 256	1 x 1 x 1	1	180	6:31
	Axial 2D TSE inversion recovery (IR) sequence with phase-sensitive reconstruction (PSIR)	7304	13	240x180	0.5 × 0.5 × 2	1	75	11:27
	Susceptibility-weighted imaging (SWI)	16	23	240 × 180	1 × 1 × 1 (reconstructed to 0.5 × 0.5 × 0.5)	1	270	6:24
<i>Cervical Cord</i>	Sagittal PD/T2weighted TSE	4000	15/80	256 x 160	1.0 x1.0 x 3.0	2	12	5:44
	Fat-suppressed 3D slab-selective fast field echo sequence (FFE)	23	5	240 x 180	0.5 x 0.5 x 5	8	11	15:58
	DTI	4000	52	64 x 48	1 x 1 x 5	1	10	08:30
<i>Optic nerve</i>	Coronal-oblique fat-suppressed 2D T2-weighted TSE	3000	80	160x160	0.5 × 0.5 x 3	1	20.3	6.30 (for each eye)
	Coronal-oblique MTR	49	3.5/5.8	160 × 160	0.75 × 0.75 x 3 (reconstructed to 0.5 × 0.5 x 3)	1	20	7 (for each eye)

*During the study, a major system upgrade took place (new scanner software, from release 3 to 5; new hardware, from Philips Achieva to Philips Ingenia-CX)

eTable 2: Timing of Antibody (Ab)-testing of patients with myelin oligodendrocyte glycoprotein antibody associated disease (MOGAD).

	Number (%) of MOGAD patients
Timing of Ab-testing	
Acute phase	19 (63)
Non-acute phase	9 (30)
NA	2 (7)
Site of Ab-testing	
Serum only	29 (97)
Serum and CSF	1 (3)
Relationship of Ab-testing with steroid treatment	
Before treatment	24 (80)
After treatment	4 (13)
NA	2 (7)
Repeated Ab-testing	
Persistence of positivity	10 (33)
Not performed	20 (67)